论著·基础医学

维莫德吉通过BRD9介导的PD-L1调控基底细胞癌微环境

王 皓,张 磊,李君龙,李欣童,孙美艳 吉林医药学院检验学院,吉林吉林

［摘要］ **目的** 探讨维莫德吉(vismodegib,Vis)通过染色质重塑因子BRD9影响基底细胞癌(basal cell carcinoma, BCC)发生发展的分子机制,分析BRD9在BCC中的表达特征及其与免疫检查点PD-L1及刺猬蛋白(Hedgehog,Hh)信号通路的关系。**方法** ①通过SKH-1无毛背景的Ptch1$^{+/-}$;LacZ报告基因小鼠构建紫外线B(ultraviolet B,UVB)诱导的BCC模型,并给予Vis干预。通过X-gal染色、免疫组化、免疫荧光和Western blot检测肿瘤组织中BRD9与PD-L1的表达与定位,并评估免疫细胞浸润。②体外以小鼠BCC的ASZ001细胞株(简称ASZ细胞)进行Vis与BRD9降解剂(dBRD9)处理,并构建BRD9过表达细胞株;检测细胞活力及BRD9、PD-L1、Gli1、Ccnd1的蛋白与mRNA表达。同时开展染色质免疫沉淀-定量聚合酶链反应,在PD-L1启动子近端(P1)与上游活跃片段(P2)检测BRD9与H3K27ac的富集变化。**结果** ①组织水平发现BRD9在BCC中呈显著阳性表达,肿瘤区域可见BRD9与PD-L1的共定位及免疫细胞浸润;而Vis显著抑制UVB诱导的小鼠BCC形成(P<0.01),降低大体积肿瘤发生率并减少X-gal阳性病灶面积(P<0.000 1),并下调BRD9的表达(P=0.024 9),减弱免疫细胞浸润。②细胞水平发现Vis处理降低ASZ细胞活力,下调BRD9、Gli1、Ccnd1的表达(P<0.000 1);dBRD9剂量依赖性抑制ASZ细胞活力,并降低PD-L1、Gli1、Ccnd1表达(P<0.000 1);BRD9过表达则提高上述分子水平(P<0.000 1)。ASZ细胞中BRD9与H3K27ac在PD-L1启动子P1/P2位点富集,经dBRD9或Vis处理后,P1/P2位点的BRD9与H3K27ac富集水平均降低(P<0.000 1)。**结论** BCC中BRD9维持PD-L1近端染色质活化并调节Hh/Gli1信号,促进免疫逃逸,Vis通过抑制Hh-BRD9-PD-L1通路重塑基底细胞癌微环境。

［关键词］ 基底细胞癌;维莫德吉;BRD9;PD-L1;肿瘤微环境

［中图法分类号］ R739.5;R966;R979.19 ［文献标志码］ A

Vismodegib regulates microenvironment of basal cell carcinoma *via* BRD9-mediated Hedgehog and PD-L1 signaling

WANG Hao, ZHANG Lei, LI Junlong, LI Xintong, SUN Meiyan College of Medical Laboratory Science, Jilin Medical University, Jilin, Jilin, China

［**Abstract**］ **Objective** To investigate how vismodegib (Vis) influences the pathogenesis of basal cell carcinoma (BCC) *via* a chromatin remodeling factor, bromodomain containing protein 9 (BRD9), and to analyze the expression profile of BRD9 in BCC and its relationship with the immune checkpoint, programmed cell death-1 ligand 1 (PD-L1) and the Hedgehog (Hh) signaling pathway. **Methods** ① A UVB-induced BCC model was established in SKH-1 hairless background Ptch1$^{+/-}$; LacZ reporter mice. Then the mice were treated with Vis, and those without treatment served as control. X-gal staining, immunohistochemistry (IHC)

［基金项目］ 吉林省自然科学基金面上项目(YDZJ202301ZYTS442);吉林省重点研发项目(20240305094YY);吉林省大学生创新创业训练计划项目(S202313706019)

［通信作者］ 孙美艳,E-mail: sunmy990@163.com

2097-0927/Copyright © 2025, 陆军军医大学(第三军医大学)。这篇开放获取文章遵循 CC BY 许可协议 (https://creativecommons.org/licenses/by/4.0/)

引用格式:王皓,张磊,李君龙,等. 维莫德吉通过BRD9介导的PD-L1调控基底细胞癌微环境[J]. 陆军军医大学学报,2025,47(21):2641-2651. DOI:10.16016/j.2097-0927.202508025.

Citation: WANG H, ZHANG L, LI J L, *et al*. Vismodegib regulates microenvironment of basal cell carcinoma *via* BRD9-mediated Hedgehog and PD-L1 signaling[J]. J Army Med Univ, 2025, 47(21): 2641-2651. DOI: 10.16016/j.2097-0927.202508025.

staining, immunofluorescence (IF) assay, and Western blotting were used to assess the expression and localization of BRD9 and PD-L1 in tumor tissues and to evaluate immune-cell infiltration. ② *In vitro*, mouse BCC cell line ASZ001 (ASZ cells) were treated with Vis or a BRD9 degrader (dBRD9), and BRD9-overexpressing cells were generated. Cell viability and the protein and mRNA levels of BRD9, PD-L1, Gli1, and cyclin D1 (Ccnd1) were measured. ChIP-qPCR was performed to examine BRD9 and H3K27ac enrichment at the PD-L1 promoter, including the promoter-proximal site (P1) and an upstream active segment (P2). **Results** ① At the tissue level, BRD9 was highly expressed in BCC, and co-localization of BRD9 and PD-L1 was observed within tumor regions, with evident immune-cell infiltration. Vis markedly suppressed UVB-induced BCC formation, reduced the probability of large-volume tumors (by probability-density analysis), decreased the X-gal-positive lesion area(P<0.000 1), down-regulated BRD9(P=0.024 9), and attenuated immune-cell infiltration. ② At the cellular level, Vis treatment reduced cell viability and down-regulated BRD9, Gli1, and Ccnd1 in ASZ cells(P<0.000 1). dBRD9 inhibited ASZ cell viability in a dose-dependent manner and decreased PD-L1, Gli1, and Ccnd1(P<0.000 1), whereas its overexpression increased the expression of these molecules(P<0.000 1). In ASZ cells, BRD9 and H3K27ac were enriched at the PD-L1 promoter P1/P2 regions. Treatment with dBRD9 or Vis reduced BRD9 and H3K27ac enrichment at P1/P2 regions(P<0.000 1). **Conclusion** In BCC, BRD9 maintains chromatin activation at the proximal PD-L1 promoter and modulates Hh/Gli1 signaling, thereby promoting immune evasion. Vis remodels the tumor immune microenvironment by inhibiting the Hh-BRD9-PD-L1 axis.

[**Key words**] basal cell carcinoma; vismodegib; BRD9; PD-L1; tumor microenvironment

Supported by the General Program of Natural Science Foundation of Jilin Province (YDZJ202301ZYTS442), the Key Research and Development Project of Jilin Province (20240305094YY), and the College Student Innovation and Entrepreneurship Training Program of Jilin Province (S202313706019).
Corresponding author: SUN Meiyan, E-mail: sunmy990@163.com

基底细胞癌(basal cell carcinoma, BCC)是常见的皮肤恶性肿瘤之一,占所有皮肤恶性肿瘤的75%以上[1]。据统计,全球范围内每年约有500万例非黑色素瘤新发病例,其中大部分为BCC[2]。在中国,随着人们生活方式的变化及皮肤病理诊断水平的提升,BCC的发病率逐年上升,成为我国皮肤科临床中常见的皮肤肿瘤类型[3-4]。有研究表明,BCC在我国南方沿海地区发病率相对较高,可能与强烈紫外线照射及人群皮肤类型相关[5]。当前BCC的临床治疗手段以手术切除为主,然而对于病灶广泛、复发性或不可手术切除的病例,缺乏有效的药物治疗选择[6]。

在分子水平上,刺猬蛋白(Hedgehog,Hh)信号通路的异常激活被认为是BCC发生与进展的核心驱动因素[7]。该通路的关键抑癌基因PTCH1常在BCC中发生突变失活,从而解除对平滑受体蛋白(smoothened,SMO)的抑制,启动Gli1转录因子并激活多种下游致癌基因[8-9]。SMO抑制剂维莫德吉(vismodegib,Vis)虽已应用于BCC治疗,但疗效有限且存在原发性与获得性耐药[10],其中SMO变体可解释相当比例的耐药病例[11],临床病例亦发现换药或联合治疗对克服耐药具有较好效果[10,12],提示除Hh通路外仍存在关键致癌环节亟待挖掘。

染色质重塑因子BRD9作为SWI/SNF复合体的重要组成,广泛参与多种肿瘤的发生与免疫逃逸过程,其异常表达与恶性进展密切相关[13-14]。此外,PD-L1作为免疫检查点蛋白,其表达受多种信号通路及表观调控因子共同调控[15]。在皮肤癌中PD-L1可介导T细胞免疫抑制,促进肿瘤逃逸[16],但其在Hh通路高活化背景下的调控机制尚未明确。已有报道提示BRD9或参与调节免疫微环境[17],本研究旨在揭示Vis作用下BRD9在BCC中的功能及其与PD-L1的关联,拓展对BCC致癌机制的理解,并为耐药病例的靶向免疫治疗提供潜在解决方案。

1 材料与方法

1.1 实验动物及分组

本实验选用购自Jackson实验室的10只6周龄雄性Ptch1$^{+/-}$;LacZ报告基因小鼠(SKH-1无毛背景),体质量21~22 g,该小鼠品系以Ptch1基因杂合背景引入LacZ报告基因构建,可通过β-半乳糖苷酶染色对BCC进行示踪[18]。采用简单随机分组,将小鼠分为(n=5):对照组(Con组)和Vis处理组(Vis组)。实验动物饲养

于吉林医药学院SPF级动物实验室,环境温度维持在22~25 ℃,湿度50%~60%,给予标准灭菌饲料和饮用水,自由摄食。动物许可证号为:SCXK(吉)2022-0001,所有实验过程通过吉林医药学院伦理委员会审批(2025-LW004)。

1.2 紫外线照射与药物干预

小鼠于实验开始后接受紫外线B(ultraviolet B,UVB)照射诱导皮肤BCC形成。UVB每次照射强度为180 mJ/cm^2,每周3次,连续8周。Vis配制于0.5%HPMC+0.1%Tween-80的无菌水溶液中。自首次UVB照射起,Vis组按20 mg/kg Vis灌胃给药,每周3次,连续8周。Con组给予等体积灌胃溶剂(0.5%HPMC+0.1%Tween-80),频次周期与Vis组一致,药物处理持续至实验结束。实验过程中第3周起,每周记录一次背部皮肤肿瘤的形成情况,通过游标卡尺测量每只小鼠背部可见肿瘤的最大长径(L)和垂直短径(W),并计算肿瘤体积(V),用于评估肿瘤生长进程及药物干预效果。肿瘤体积的计算公式为:$V=\frac{L\times W^2}{2}$。

1.3 细胞培养、转染、筛选及分组

实验所用细胞为源自小鼠BCC的ASZ001细胞株(简称ASZ细胞),于37 ℃、5%CO_2恒温培养箱中,以含10%胎牛血清和1%青链霉素的DMEM完全培养基进行常规培养。为构建BRD9过表达模型,使用慢病毒系统将BRD9基因导入ASZ细胞。所用慢病毒载体为{pLV[Exp]-Hygro-CMV>mBrd9NM_001378947.1/FLAG:T2A:mCherry},由上海吉凯基因公司合成并包装。该载体在CMV启动子驱动下表达FLAG标签的小鼠BRD9,同时通过T2A元件共表达mCherry荧光蛋白用于阳性筛选,并携带Hygromycin抗性基因。转染前,ASZ细胞接种于6孔板中,待细胞密度达40%~50%时,加入含病毒颗粒的感染液,按感染复数(multiplicity of infection,MOI)为10进行感染,并配合8 μg/mL Polybrene(Sigma-Aldrich,美国)增强感染效率。24 h后更换为新鲜完全培养基,48 h后添加100 μg/mL Hygromycin B(Invitrogen,美国)进行抗性筛选,连续筛选7 d,获得稳定表达BRD9的细胞株(命名为ASZ-BRD9),并检测细胞活力及过表达效果。对数生长期的ASZ细胞按1∶1∶1随机分为:对照(ASZ)组加入等体积载体(DMSO,终浓度为0.1%);dBRD9(ASZ-dBRD9)组通过BRD9降解剂(dBRD9,10.0 nmol/L)处理24 h;Vis(ASZ-Vis)组通过Vis(10 μmol/L)处理24 h。除药物外其余培养条件一致,DMSO终浓度在各组为0.1%,通过染色质免疫沉淀-定量聚合酶链反应(chromatin immunoprecipitation quantitative polymerase chain reaction,ChIP-qPCR)分析。

1.4 细胞活力检测

采用细胞计数试剂盒(CCK-8,Dojindo,日本)检测Vis对ASZ细胞活力的影响。将ASZ细胞以5×10^{3}个/孔的密度接种于96孔板中,贴壁后分别给予不同处理,其中Vis浓度为0、0.01、0.10、1.00、5.00、10.00、20.00、40.00 μmol/L,处理时间为24、48和72 h。BRD9降解剂(dBRD9)处理浓度为0、0.5、5.0、10.0、100.0、250.0、500.0和1 000.0 nmol/L,处理时间为24 h。每组设3个复孔。处理结束后,每孔加入10 μL CCK-8工作液,孵育2 h。通过酶标仪于450 nm波长处测定*OD*(450)值,以评估细胞活力。实验重复3次,并采用GraphPad Prism 10.0软件计算半数抑制浓度(half maximal inhibitory concentration,IC_{50})。

1.5 免疫组化(immunohistochemistry,IHC)染色

小鼠经最后一次UVB照射后24 h在异氟烷麻醉下处死,自背部受照区域切取皮肤标本(含表皮、真皮及部分皮下组织,约8 mm×8 mm)。组织立即置于10%中性甲醛室温固定24 h,随后经梯度乙醇脱水、二甲苯透明后石蜡包埋,制备5 μm厚度的石蜡切片。切片脱蜡、复水后进行抗原修复(柠檬酸缓冲液pH=6.0,微波加热15 min),3%H_2O_2室温孵育15 min以阻断内源性过氧化物酶,5%BSA封闭1 h。随后加入一抗(抗BRD9,PA5-113488,Invitrogen,美国,1∶500)于4 ℃孵育过夜。第2天PBS洗涤后加入HRP标记的二抗,室温孵育1 h。经DAB显色、苏木素复染后脱水封片。切片经光学显微镜观察并拍照分析。

1.6 X-gal染色实验

取上述IHC步骤中制作的皮肤组织切片进行X-gal染色以检测β-半乳糖苷酶活性。组织切片经IHC步骤中的脱蜡复水后,在X-gal染色液[含5 mmol/L $K_3Fe(CN)_6$、5 mmol/L $K_4Fe(CN)_6$、2 mmol/L $MgCl_2$和1 mg/mL X-gal,溶于PBS]中于37 ℃避光孵育16 h。经常规苏木精-伊红(hematoxylin and eosin,HE)复染并脱水封片,镜下观察并拍照记录。

1.7 Western blot分析

皮肤组织及细胞经RIPA裂解液(含蛋白酶抑制剂)匀浆裂解后,在4 ℃下以12 000 r/min离心10 min,取上清并进行BCA蛋白定量,每孔加样30~50 μg蛋白,于10%SDS-PAGE凝胶电泳分离后转膜至PVDF膜。5%脱脂奶粉/TBST封闭1 h,加入一抗(抗BRD9:

PA5-113488, Invitrogen, 美国, 1∶1 000; 抗 Cyclin D1: 2978, Cell Signaling, 美国, 1∶2 000; 抗 PD-L1: 13684, Cell Signaling, 美国, 1∶1 000; 抗 Gli1: 2643, Cell Signaling, 美国, 1∶1 000)于4 ℃孵育过夜。TBST洗膜3次,每次10 min,加入HRP标记的二抗于室温孵育1 h。ECL发光液显影并使用成像系统检测蛋白条带。

1.8 RT-qPCR检测

使用TRIzol试剂(Invitrogen, 美国)从ASZ细胞中提取总RNA, 按照SuperScript™ Ⅲ First-Strand Synthesis System(Thermo Fisher, 美国)试剂盒说明进行反转录反应,将RNA反转录为cDNA。qPCR反应采用2×SYBR Green PCR Master Mix(TaKaRa, 日本)进行扩增,使用LightCycler®96 Real-Time PCR System(Roche, 德国)完成实时荧光定量检测。每个样本设3个技术重复孔,以β-actin作为内参基因,采用$2^{-\Delta\Delta Ct}$方法计算相对表达量。所用引物由生工生物工程(上海)股份有限公司合成,引物序列见表1。

表1 RT-qPCR引物序列

Table 1 RT-qPCR primer sequences

Genes	Sequences(5′→3′)
β-actin	Forward primer: CATCCTGCGTCTGGACCTG
	Reverse primer: ATCTCCTTCTGCATCCTGTC
BRD9	Forward primer: CTCAGACCACGAACGGGAG
	Reverse primer: TTCCAGGGTCGAAAGCATCAG
Gli1	Forward primer: CCAAGCCAACTTTATGTCAGGG
	Reverse primer: AGCCCGCTTCTTTGTTAATTTGA
Ccnd1	Forward primer: AGCTGTGCATCTACACCGAC
	Reverse primer: TGTGAGGCGGTAGTAG

1.9 免疫荧光染色

皮肤组织切片经IHC步骤中的脱蜡复水、抗原修复及封闭后,加入一抗混合液[兔抗-BRD9(PA5-113488, Invitrogen, 1∶100)和鼠抗-PD-L1(66248-1-Ig, Proteintech, 1∶200); 兔抗-Foxp3(12653, Cell Signaling, 1∶200)和鼠抗-CD4(555349, BD Biosciences, 1∶100)],置于湿盒中4 ℃孵育过夜。次日回温并用PBS洗涤3次,每次5 min,分别孵育相应的荧光标记二抗(Alexa Fluor 488标记的兔抗IgG和Alexa Fluor 594标记的鼠抗IgG),室温避光孵育1 h。再次PBS洗涤后,用DAPI染核5 min,PBS洗净,封片后通过激光共聚焦显微镜(Leica STELLARIS 5)拍照观察。

1.10 ChIP-qPCR检测

ASZ细胞按1.3实验分组(Con、ASZ-dBRD9、ASZ-Vis)处理后进行ChIP,设置同源正常IgG作为阴性对照。1%甲醛室温交联10 min,125 mmol/L glycine终止5 min。PBS洗涤后收集细胞,于含蛋白酶抑制剂的裂解液中裂解;将染色质超声至200~500 bp,在4 ℃下以8 000 r/min离心取上清,各样本留出1%作为Input;4 ℃旋转孵育过夜,加入anti-BRD9(PA5-113488, Invitrogen, 美国, 1∶200)、anti-H3K27ac(ab4729, Abcam,美国,1∶500);次日加入Protein A/G磁珠继续孵育2 h;依次用低盐、高盐、LiCl洗液及TE洗脱后65 ℃过夜逆交联,并依次RNase A(37 ℃, 30 min)、Proteinase K(55 ℃, 1 h)处理;柱式试剂盒纯化DNA,qPCR条件参照1.8;针对PD-L1启动子设置3个位点:上游活跃片段P2(−523~−436 bp)、启动子近端P1(−58~+41 bp)、N(+799~+937 bp);引物序列见表2。

表2 ChIP-qPCR引物序列

Table 2 ChIP-qPCR primer sequences

Genes	Sequences(5′→3′)
PD-L1ChIP1	Forward primer: GCTGTAGAGGAAGGCAACCTATGTG
	Reverse primer: TTTGGGTGGGAGTGGAACCTGAGG
PD-L1ChIP2	Forward primer: ACCTAAACTGAAAGCTTCCGC
	Reverse primer: CCCAAGGCAGCAAATCCAGT
PD-L1ChIP3	Forward primer: GCTGATGATGATAGTGACCAAGCG
	Reverse primer: CCTGAACCCTGTGCTCAAATCC

1.11 统计学分析

使用GraphPad Prism 10.0进行统计分析。结果采用$\bar{x}\pm s$表示,两组间比较采用独立样本t检验,3组及以上比较采用单因素方差分析(one-way ANOVA),$P<0.05$表示差异有统计学意义。

2 结果

2.1 Vis抑制Ptch1$^{+/-}$小鼠UVB诱导的BCC形成并下调BRD9表达

为了评估Vis对UVB诱导的BCC形成的抑制作用,本研究基于Ptch1$^{+/-}$背景的SKH-1无毛小鼠模型,通过连续UVB照射构建皮肤肿瘤模型,并在此过程中给予Vis药物干预,以分析皮肤肿瘤发生情况及相关分子表达变化。如图1A所示,Vis组小鼠皮肤表面肿瘤体积明显小于Con组。进一步通过肿瘤面积的概率密度函数分析发现,Vis能显著降低大体积肿瘤的发生率;以每只小鼠病灶体积中位数汇总后分析发现,Vis组肿瘤体积显著缩小($P<0.001$,图1B),提示其在该模型中具有良好的抗肿瘤作用。X-gal染色结果显示,Con组皮肤中可见多个X-gal阳性信号聚集的BCC

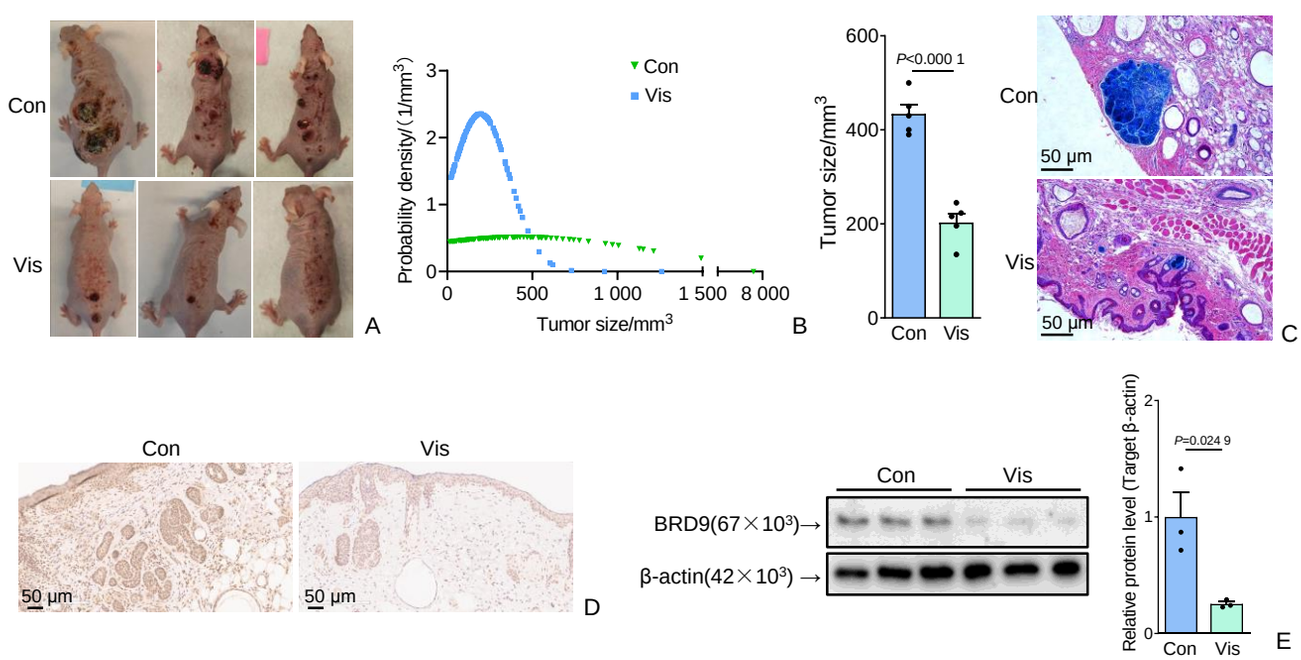
样病灶,而Vis组中阳性染色区域显著减少(P<0.000 1,图1C),进一步支持Vis具有抑制BCC形成的作用。为探究该作用潜在的分子机制,进一步检测皮肤肿瘤组织中BRD9的表达水平。IHC分析显示BRD9在Con组肿瘤区域呈显著阳性表达,而在Vis组中显著减弱(图1D)。Western blot分析结果表明,Vis处理后BRD9蛋白表达水平显著下调(P=0.024 9,图1E)。上述结果提示BRD9可能在BCC的发生发展过程中发挥促进作用,其表达可能受Vis抑制的Hh信号通路调控。

2.2　Vis通过抑制Hh/BRD9通路显著抑制ASZ细胞增殖能力

为进一步验证Vis对BCC的作用机制,本研究利用BCC细胞系ASZ评估其细胞毒性及其对关键信号分子的调控作用。细胞活力检测结果显示,Vis对ASZ细胞呈浓度和时间依赖性抑制作用,随着处理时间延长,其IC_{50}逐渐下降,24、48及72 h的IC_{50}分别为7.326、3.842和0.910 μmol/L(图2A)。本研究检测了BRD9蛋白在不同剂量Vis处理下的表达变化。Western blot分析显示,BRD9表达水平随药物浓度升高逐渐降低(P<0.000 1),40 μmol/L时完全被抑制(图2B)。进一步在细胞水平及组织水平检测BRD9下游分子Gli1和Ccnd1的表达变化,结果表明Vis处理显著下调这2种蛋白的表达(P<0.001,图2C、D),提示其可能抑制Hh信号通路进而负向调控BRD9表达,抑制其介导的下游促增殖通路,从而发挥抗肿瘤作用。

2.3　BRD9在BCC中促进肿瘤进展并调控Hh通路及PD-L1表达

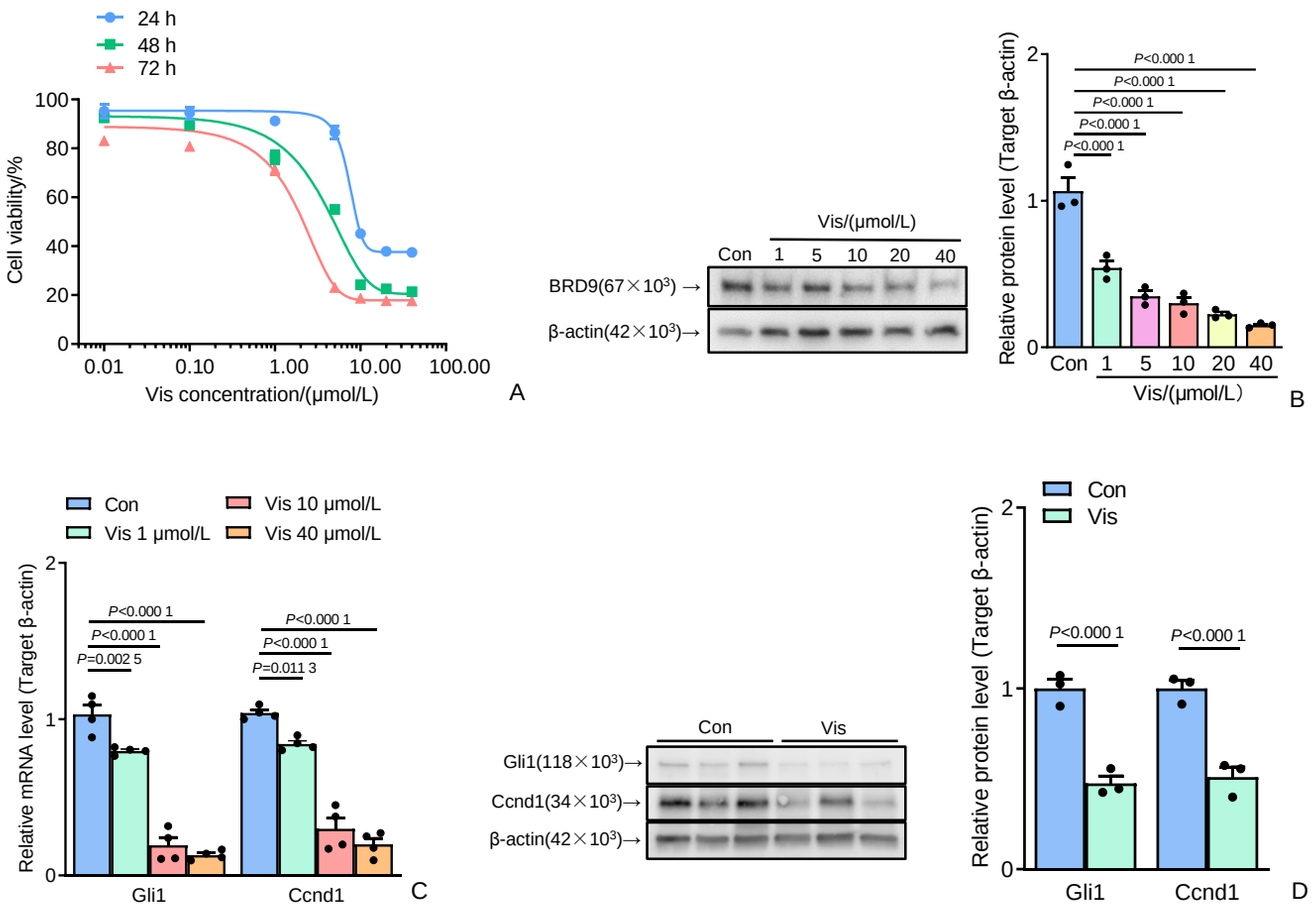
本研究进一步探究了BRD9在BCC发生发展中的功能及其信号机制。ASZ细胞经不同浓度的BRD9降解剂dBRD9处理24 h后,细胞活力呈剂量依赖性下降(图3A),提示dBRD9具有一定程度的抗肿瘤潜力。Western blot结果显示,与Con组相比,dBRD9处理显著下调BRD9蛋白表达,同时伴随Ccnd1、PD-L1和Gli1等关键增殖和免疫调控分子表达的降低(P<0.01,图3B),提示BRD9可能调控肿瘤细胞的增殖与免疫逃逸能力。为进一步验证BRD9的功能,本研究构建了BRD9过表达质粒并转染ASZ细胞(图3C)。BRD9过表达显著增强ASZ细胞中BRD9、PD-L1和Ccnd1蛋白表达(P<0.05,图3D),RT-qPCR结果也显示BRD9及其下游靶点Gli1的mRNA表达上调(P<0.000 1,图3E)。在此基础上,采用ChIP-qPCR检测PD-L1启动子区域3个位点的富集情况。结果显示,在ASZ细胞



A: Representative gross images of skin tumor burden in Con and Vis-treated mice (n=5); B: Probability-density plots of tumor area and groupwise tumor area analysis for Con and Vis-treated mice (n=5); C: X-gal staining of BCC-like lesions in skin sections from Con and Vis-treated groups; D: Immunohistochemical results for BRD9 in tumor tissues from Con and Vis-treated groups; E: Western blot analysis for BRD9 in mouse tumor tissues with densitometric quantification (n=3)

图1　Vis对UVB诱导的小鼠基底细胞癌表型及BRD9表达的影响

Figure 1　Effects of vismodegib (Vis) on the phenotype of UVB-induced mouse basal cell carcinoma and BRD9 protein expression



A: Cell viability of ASZ cells across Vis concentrations and time points assessed by CCK-8 assay, with IC_{50} estimation (n=6); B: Western blot analysis of BRD9 in ASZ cells treated with the indicated Vis concentrations, with densitometric quantification (n=3); C: RT-qPCR analysis of Gli1 and Ccnd1 mRNA levels in Vis-treated versus control ASZ cells (n=4); D: Western blot analysis of Gli1 and Ccnd1 in mouse tumor tissues after Vis treatment, with densitometric quantification (n=3)

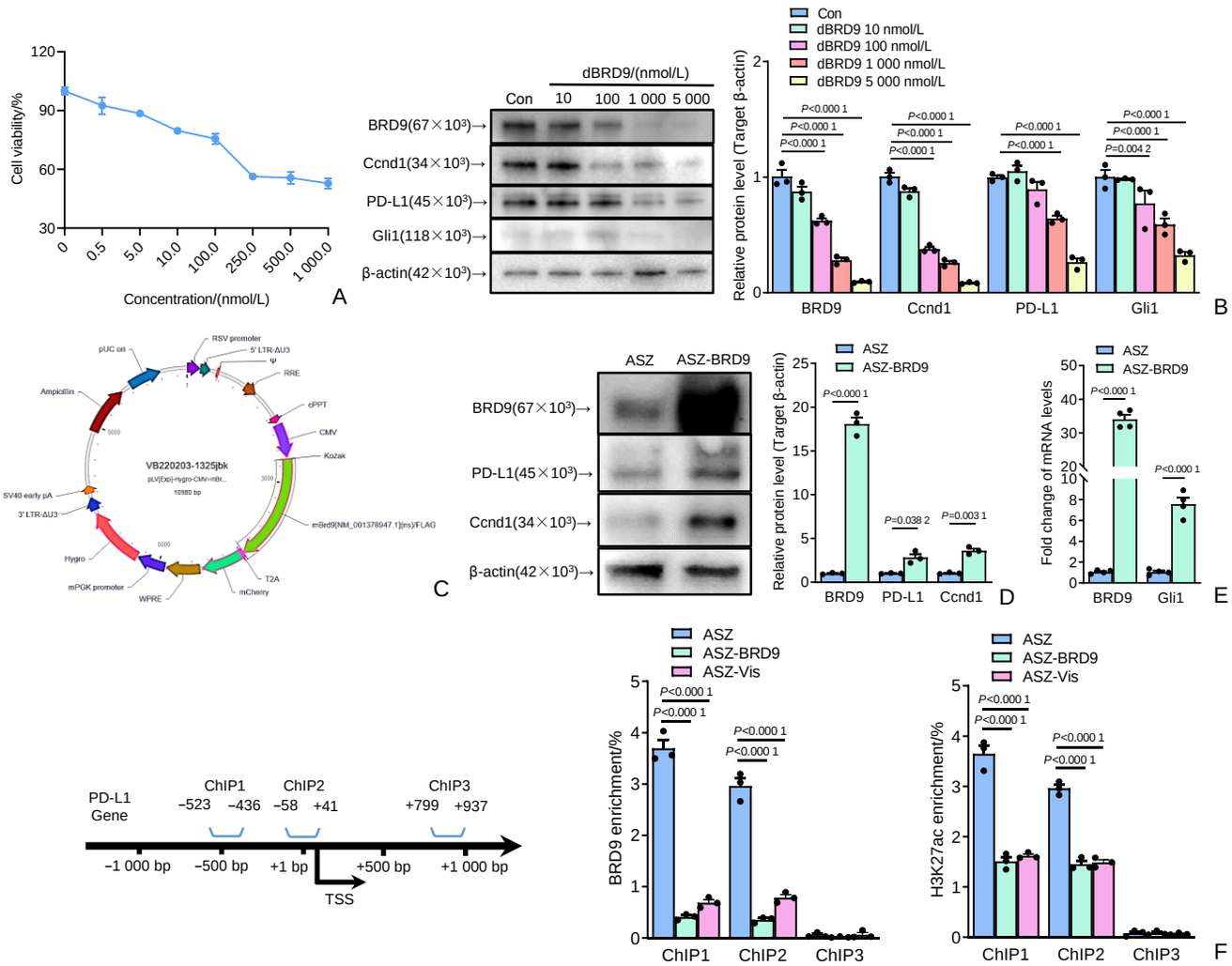
图 2 Vis抑制ASZ细胞增殖并下调BRD9及其下游分子表达

Figure 2 Vismodegib(Vis) inhibits cell proliferation and down-regulates BRD9 and its downstream effector molecules in ASZ cells

中,BRD9与H3K27ac在ChIP1/ChIP2处均有富集,而在阴性对照的ChIP3处接近背景;经dBRD9或Vis处理后,ChIP1/ChIP2处的BRD9与H3K27ac富集水平均显著降低(P<0.000 1,图3F)。以上结果表明,BRD9可能通过调控Hh通路并维持PD-L1启动子近端的染色质活化,从而促进BCC的发生发展,为其作为潜在治疗靶点提供实验依据。

2.4 Vis处理对小鼠BCC中BRD9/PD-L1表达及免疫细胞分布的影响

免疫荧光染色结果显示,在UVB处理后Con组小鼠皮肤组织的BRD9和PD-L1均明显表达,其中BRD9的表达更为显著,在表皮和真皮组织中均有表达。图中箭头所示为二者在肿瘤周围区域存在的共定位现象;且经Vis处理后,组织中BRD9和PD-L1表达水平明显下降(图4A)。本研究进一步分析免疫相关细胞的分布情况,结果发现Con组中调节性T细胞标志物Foxp3$^+$ Treg与CD4$^+$ T细胞均显著聚集于肿瘤区域,而Vis处理显著减少了肿瘤微环境中Foxp3$^+$ Treg细胞及CD4$^+$ T细胞的浸润(图4B)。HE结果显示,Con组可见典型BCC胞巢,肿瘤及其周围间质内以小淋巴细胞为主的炎性细胞明显聚集;而Vis处理后,肿瘤巢体量/数量减少,瘤旁炎性细胞明显稀少(图4C)。结合图1D的IHC结果(表皮BRD9表达未见显著变化),可基本排除正常表皮BRD9的干扰,提示上述浸润变化发生于肿瘤/瘤旁区域,并与肿瘤组织BRD9下调相关,表明Vis在降低BRD9/PD-L1表达的同时,伴随肿瘤区域及瘤旁区域免疫细胞浸润的下降,从而重塑肿瘤免疫微环境。



A: Cell viability of ASZ cells after 24 h treatment with increasing concentrations of dBRD9 (n=6); B: Western blot analysis of BRD9, Ccnd1, PD-L1, and Gli1 in ASZ cells treated with dBRD9, with densitometric quantification (n=3); C: Schematic diagram of the BRD9 overexpression plasmid; D: Western blot analysis of BRD9, PD-L1, and Ccnd1 following BRD9 overexpression in ASZ cells, with densitometric quantification (n=3); E: RT-qPCR analysis of BRD9 and Gli1 mRNA levels after BRD9 overexpression in ASZ cells (n=4); F: ChIP-qPCR showing BRD9 and H3K27ac enrichment at 3 sites within the PD-L1 promoter after dBRD9 or Vis treatment (n=3)

图3 BRD9降解及过表达对ASZ细胞中相关信号通路分子表达的影响

Figure 3 Effects of BRD9 degradation and overexpression on Hedgehog pathway effectors in ASZ cells

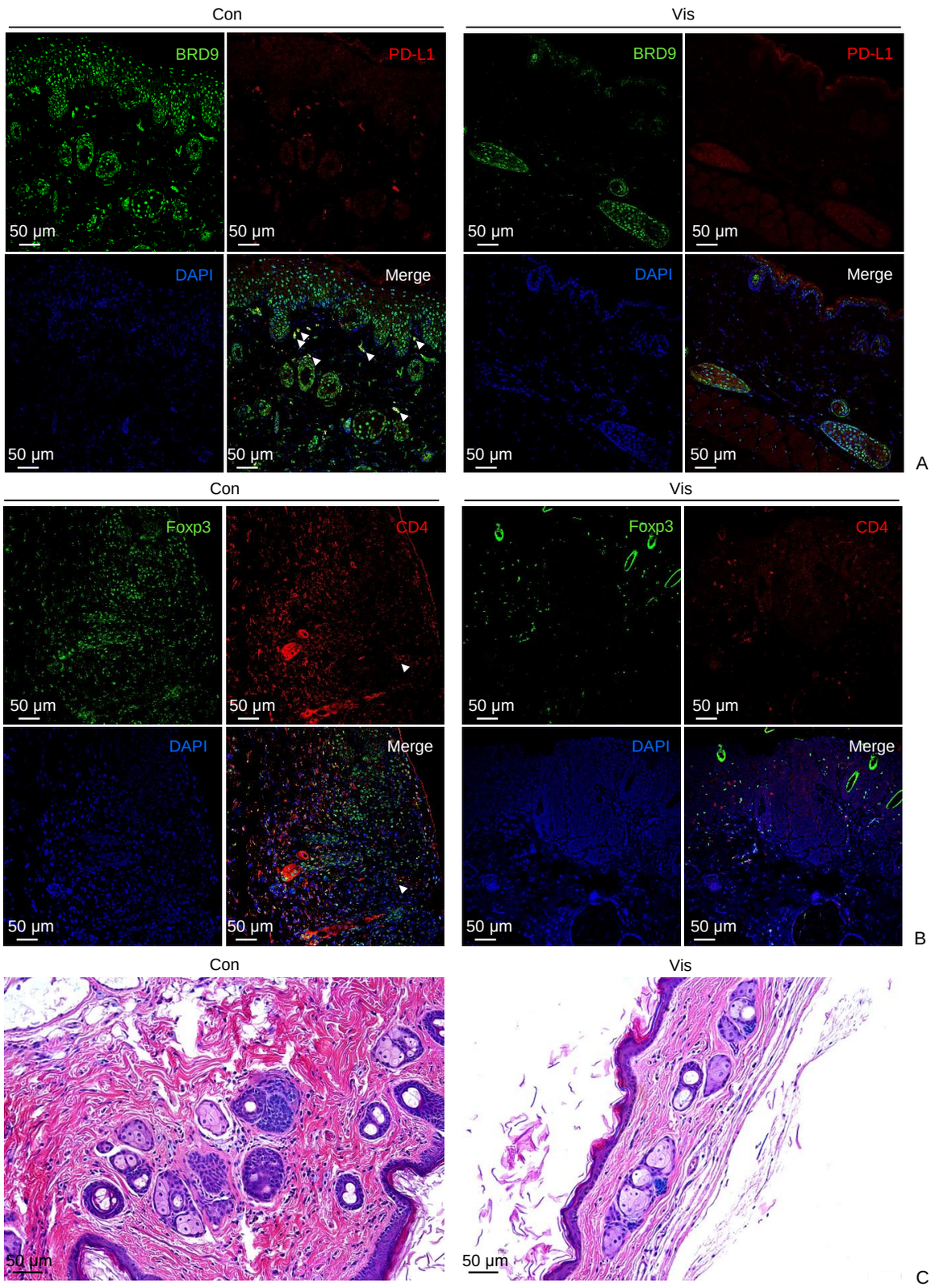
3 讨论

3.1 BRD9在肿瘤中的作用与意义

本研究从机制层面探讨了Vis抑制BRD9介导的免疫逃逸通路在BCC发生发展中的作用。已有研究表明,BRD9作为SWI/SNF染色质重塑复合物的辅助亚基,广泛参与染色质开放、转录激活等多种生物学过程,在肿瘤细胞中的表达常显著上调,并与多种癌症的增殖、迁移及免疫逃逸密切相关[19-20]。泛癌分析也显示,BRD9在肺癌、肝癌、乳腺癌等实体瘤中高表达,且与患者不良预后显著相关[13]。

3.2 免疫检查点PD-L1与联合治疗需求

PD-L1是重要的免疫检查点蛋白,其高表达常见于包括黑色素瘤、非小细胞肺癌、肾癌等多种恶性肿瘤,并已成为多个实体瘤中免疫治疗的核心靶点[21]。近年来,免疫治疗尤其是抗PD-1/PD-L1单抗在多种肿瘤中的应用带来了革命性进展。一些此类免疫药物已获得美国食品药品监督管理局(Food and Drug Administration,FDA)批准上市,如治疗肺癌的纳武利尤单抗和帕博利珠单抗,以及用于乳腺癌的阿特珠单



A: Immunofluorescence assay of skin sections from Con and Vis-treated mice showing BRD9 (green), PD-L1 (red), and their co-localization; nuclei counterstained with DAPI (blue); B: Immunofluorescence assay showing $Foxp3^+$ regulatory T cells (green) and $CD4^+$ T cells (red) in Con and Vis groups; nuclei counterstained with DAPI (blue); C: HE staining of skin sections from Con and Vis groups

图4 Vis处理后小鼠BCC中BRD9/PD-L1及Foxp3/CD4的免疫荧光双标染色

Figure 4 Dual immunofluorescence staining for BRD9/PD-L1 and Foxp3/CD4 in mouse BCC after vismodegib (Vis) treatment

抗[22-24]。然而,这些药物的治疗效果有限,部分患者存在原发性或获得性耐药[25],提示免疫治疗的单药策略仍有不足,需进一步探索联合治疗机制和耐药调控靶点。有研究发现,BRD9可通过影响肿瘤免疫微环境中髓源性抑制细胞浸润,调节PD-L1表达,并预测抗PD-1治疗患者的生存预后,提示其在免疫治疗响应中具有潜在调控作用[13,26]。GEO数据集分析进一步表明,BRD9的表达在接受免疫治疗的黑色素瘤患者中具有良好的预后预测价值,提示其可能参与调控PD-L1介导的免疫逃逸,并作为潜在免疫治疗敏感性标志物[13]。Vis也已获FDA批准,用于治疗局部晚期或转移性BCC,成为首个靶向Hh通路的上市药物[27]。然而,关于Vis的药物作用机制尚不完全清楚,对于其是否可以通过介导BRD9调控PD-L1的表达,尚缺乏明确的实验证据。

3.3 BRD9与PD-L1的关联及表观机制推测

本研究在BCC模型中发现,BRD9与PD-L1在组织层面呈共表达趋势,且通过BRD9小分子抑制剂处理或过表达干预均可显著影响PD-L1的表达水平,提示BRD9可能通过表观遗传机制(如染色质重塑)促进PD-L1的转录,从而增强肿瘤免疫逃逸能力。这一发现具有重要意义:①揭示了BRD9与免疫检查点调控之间可能存在的功能关联,打破了传统上BCC被认为免疫原性较低的固有观念,提示即便在低免疫原性肿瘤中也可能存在可靶向的免疫逃逸机制[28];②为后续将BRD9抑制剂与免疫检查点抑制剂联合应用于BCC治疗提供了理论依据,为皮肤癌等实体瘤的联合免疫治疗提供了潜在新靶点。此外,本研究发现BRD9与PD-L1在组织层面呈共表达趋势。鉴于BRD9是ncBAF的标志性亚基参与染色质开放/增强子活化的已知功能[29],推测BRD9可能通过促进PD-L1启动子/近端增强子的染色质可及性,从而增强其转录。此外,Hh/Gli1通路与炎症-干扰素信号(如IRF1/STAT1)在多肿瘤中可共同上调PD-L1[30];本研究通过ChIP-qPCR发现,BRD9与H3K27ac在PD-L1启动子近端及上游活跃片段富集;经dBRD9或Vis处理后,ChIP1/ChIP2的BRD9与H3K27ac富集水平均下降,进一步支持BRD9作为转录协同因子,在这些因子占位处提供染色质支架,导致PD-L1表达增强,从而增强肿瘤的免疫逃逸能力。

3.4 肿瘤免疫微环境变化与Hh通路关联

本研究发现Con组Treg标志物显著浸润,而Vis干预可明显减少Foxp3$^+$ Treg细胞和CD4$^+$ T细胞在肿瘤中的聚集。这一观察结果提示,Vis除了通过BRD9/PD-L1轴下调免疫检查点分子外,还可能通过削弱Treg介导的免疫抑制来调节肿瘤免疫微环境,从而间接增强抗肿瘤免疫反应。由于Treg细胞在多种肿瘤中发挥免疫抑制作用,其富集常与免疫治疗耐药相关[31],因此,Vis可能在调控Treg细胞活性方面发挥关键作用。考虑到目前Vis虽已被广泛用于BCC治疗,但仍存在部分患者耐药、缓解不彻底等问题[32],进一步靶向BRD9/PD-L1通路,有望作为新的干预途径,实现免疫微环境重塑及治疗应答率提高。此外,Vis可通过抑制Hh信号通路而间接影响多种下游分子表达[33]。本研究显示BRD9的表达水平也受到Hh通路调控,在Vis干预后显著下调,提示BRD9可能作为Hh通路的下游效应分子参与BCC发生过程,从而将经典信号通路与表观调控机制连接起来,进一步拓展了对BCC分子致癌机制的认识和理解。

综上所述,BRD9在BCC中显著表达,通过维持PD-L1启动子近端的染色质活化调节Hh/GLI1信号,调控PD-L1表达与肿瘤免疫逃逸。Vis可通过抑制Hh-BRD9-PD-L1通路发挥抗肿瘤作用并重塑肿瘤免疫微环境。

利益冲突 本文所有作者声明不存在利益冲突

参考文献:

[1] LI D, YAN G, SONG S S, *et al*. Temporal trend in non-melanoma skin cancer mortality in China, 1992-2021: an analysis for the global burden of disease study 2021[J]. Front Med, 2025, 12: 1495454. DOI:10.3389/fmed.2025.1495454.

[2] PAN Y M, TANG B, GUO Y W, *et al*. Global burden of non-melanoma skin cancers among older adults: a comprehensive analysis using machine learning approaches[J]. Sci Rep, 2025, 15(1): 15266. DOI:10.1038/s41598-025-99605-5.

[3] 国家皮肤与免疫疾病临床医学研究中心, 中国医师协会皮肤科分会. 中国皮肤基底细胞癌诊疗指南(2023版)[J]. 中华医学杂志, 2024, 104(6): 391-410. DOI:10.3760/cma.j.cn112137-20231113-01082.
National Clinical Research Center for Skin and Immunologic Diseases, Dermatologist Branch of Chinese Medical Doctor Association. Chinese guildeline on diagnosis and treatment of basal cell carcinoma (2023 edition)[J]. Natl Med J China, 2024, 104(6): 391-410. DOI: 10.3760/cma.j.cn112137-20231113-01082.

[4] KIM G K, DEL ROSSO J Q, BELLEW S. Skin cancer in asians: part 1: nonmelanoma skin cancer[J]. J Clin Aesthet Dermatol, 2009, 2(8): 39-42.

[5] KANTOR J. The epidemiology of skin cancer in Asia: September 2021[J]. J Am Acad Dermatol, 2021, 85(3):

569. DOI:10.1016/j.jaad.2021.07.008.

[6] PERIS K, FARGNOLI M C, KAUFMANN R, *et al*. European consensus-based interdisciplinary guideline for diagnosis and treatment of basal cell carcinoma-update 2023 [J]. Eur J Cancer, 2023, 192: 113254. DOI: 10.1016/j.ejca.2023.113254.

[7] PELLEGRINI C, MATURO M G, DI NARDO L, *et al*. Understanding the molecular genetics of basal cell carcinoma [J]. Int J Mol Sci, 2017, 18(11): 2485. DOI: 10.3390/ijms18112485.

[8] GAMBINI D, PASSONI E, NAZZARO G, *et al*. Basal cell carcinoma and hedgehog pathway inhibitors: focus on immune response [J]. Front Med, 2022, 9: 893063. DOI: 10.3389/fmed.2022.893063.

[9] ATWOOD S X, SARIN K Y, WHITSON R J, *et al*. Smoothened variants explain the majority of drug resistance in basal cell carcinoma [J]. Cancer Cell, 2015, 27(3): 342-353. DOI:10.1016/j.ccell.2015.02.002.

[10] DOAN H Q, CHEN L, NAWAS Z, *et al*. Switching Hedgehog inhibitors and other strategies to address resistance when treating advanced basal cell carcinoma [J]. Oncotarget, 2021, 12(20): 2089-2100. DOI: 10.18632/oncotarget.28080.

[11] SHARPE H J, PAU G, DIJKGRAAF G J, *et al*. Genomic analysis of smoothened inhibitor resistance in basal cell carcinoma [J]. Cancer Cell, 2015, 27(3): 327-341. DOI: 10.1016/j.ccell.2015.02.001.

[12] STRATIGOS A J, SEKULIC A, PERIS K, *et al*. Cemiplimab in locally advanced basal cell carcinoma after hedgehog inhibitor therapy: an open-label, multi-centre, single-arm, phase 2 trial [J]. Lancet Oncol, 2021, 22(6): 848-857. DOI:10.1016/S1470-2045(21)00126-1.

[13] CHEN Y, GAO Z T, MOHD-IBRAHIM I, *et al*. Pan-cancer analyses of bromodomain containing 9 as a novel therapeutic target reveals its diagnostic, prognostic potential and biological mechanism in human tumours [J]. Clin Transl Med, 2024, 14(2): e1543. DOI:10.1002/ctm2.1543.

[14] WANG X P, SONG C C, YE Y, *et al*. BRD9-mediated control of the TGF-β/Activin/Nodal pathway regulates self-renewal and differentiation of human embryonic stem cells and progression of cancer cells [J]. Nucleic Acids Res, 2023, 51(21): 11634-11651. DOI:10.1093/nar/gkad907.

[15] YAMAGUCHI H, HSU J M, YANG W H, *et al*. Mechanisms regulating PD-L1 expression in cancers and associated opportunities for novel small-molecule therapeutics [J]. Nat Rev Clin Oncol, 2022, 19(5): 287-305. DOI:10.1038/s41571-022-00601-9.

[16] MOUSA A M, ENK A H, HASSEL J C, *et al*. Immune checkpoints and cellular landscape of the tumor microenvironment in non-melanoma skin cancer (NMSC) [J]. Cells, 2024, 13(19): 1615. DOI: 10.3390/cells13191615.

[17] WANG G B, HUANG J B, CHEN H Q, *et al*. Exploring novel biomarkers and immunotherapeutic targets for biofeedback therapies to reveal the tumor-associated immune microenvironment through a multimetric analysis of kidney renal clear cell carcinoma [J]. Discov Oncol, 2025, 16(1): 311. DOI:10.1007/s12672-025-02090-5.

[18] WANG G Y, WANG J, MANCIANTI M L, *et al*. Basal cell carcinomas arise from hair follicle stem cells in Ptch1$^{+/-}$ mice [J]. Cancer Cell, 2011, 19(1): 114-124. DOI:10.1016/j.ccr.2010.11.007.

[19] LEE S Y, LEE S H, KWAK M J, *et al*. Depletion of BRD9-mediated R-loop accumulation inhibits leukemia cell growth *via* transcription-replication conflict [J]. Nucleic Acids Res, 2025, 53(12): gkaf613. DOI:10.1093/nar/gkaf613.

[20] HANSEN A, SANDERS C, FRONHOFFS F, *et al*. BRD9 inhibition as potential treatment option for testicular germ cell tumors [J]. Andrology, 2025. DOI: 10.1111/andr.70038. DOI:10.1111/andr.70038.

[21] GOMPELMANN D, SAROVA P, MOSLEH B, *et al*. PD-L1 assessment in lung cancer biopsies-pitfalls and limitations [J]. Int J Biol Markers, 2024, 39(1): 3-8. DOI:10.1177/03936155231214273.

[22] SUZMAN D L, AGRAWAL S, NING Y M, *et al*. FDA approval summary: atezolizumab or pembrolizumab for the treatment of patients with advanced urothelial carcinoma ineligible for cisplatin-containing chemotherapy [J]. Oncologist, 2019, 24(4): 563-569. DOI: 10.1634/theoncologist.2018-0084.

[23] TWOMEY J D, ZHANG B L. Cancer immunotherapy update: FDA-approved checkpoint inhibitors and companion diagnostics [J]. AAPS J, 2021, 23(2): 39. DOI:10.1208/s12248-021-00574-0.

[24] OLIVARES-HERNÁNDEZ A, GONZÁLEZ DEL PORTILLO E, TAMAYO-VELASCO Á, *et al*. Immune checkpoint inhibitors in non-small cell lung cancer: from current perspectives to future treatments-a systematic review [J]. Ann Transl Med, 2023, 11(10): 354. DOI:10.21037/atm-22-4218.

[25] GUO L B, WEI R, LIN Y, *et al*. Clinical and recent patents applications of PD-1/PD-L1 targeting immunotherapy in cancer treatment-current progress, strategy, and future perspective [J]. Front Immunol, 2020, 11: 1508. DOI: 10.3389/fimmu.2020.01508.

[26] ZHU Q S, GU X, WEI W, *et al*. BRD9 is an essential

regulator of glycolysis that creates an epigenetic vulnerability in colon adenocarcinoma[J]. Cancer Med, 2023, 12(2): 1572-1587. DOI:10.1002/cam4.4954.

[27] SEKULIC A, MIGDEN M R, ORO A E, *et al*. Efficacy and safety of vismodegib in advanced basal-cell carcinoma[J]. N Engl J Med, 2012, 366(23): 2171-2179. DOI: 10.1056/NEJMoa1113713.

[28] DESSINIOTI C, STRATIGOS A J. Immunotherapy and its timing in advanced basal cell carcinoma treatment[J]. Dermatol Pract Concept, 2023, 13(4): e2023252. DOI: 10.5826/dpc.1304a252.

[29] MICHEL B C, D'AVINO A R, CASSEL S H, *et al*. A non-canonical SWI/SNF complex is a synthetic lethal target in cancers driven by BAF complex perturbation[J]. Nat Cell Biol, 2018, 20(12): 1410-1420. DOI: 10.1038/s41556-018-0221-1.

[30] KOH V, CHAKRABARTI J, TORVUND M, *et al*. Hedgehog transcriptional effector GLI mediates mTOR-Induced PD-L1 expression in gastric cancer organoids[J]. Cancer Lett, 2021, 518: 59-71. DOI: 10.1016/j.canlet.2021.06.007.

[31] DĄBROWSKA A, GRUBBA M, BALIHODZIC A, *et al*. The role of regulatory T cells in cancer treatment resistance[J]. Int J Mol Sci, 2023, 24(18): 14114. DOI: 10.3390/ijms241814114.

[32] TRUONG K, PEERA M, LIU R, *et al*. Real-world data on the efficacy and safety of hedgehog pathway inhibitors in patients with basal cell carcinoma: Experience of a tertiary Australian centre[J]. Australas J Dermatol, 2024, 65(8): e248-e254. DOI:10.1111/ajd.14373.

[33] GUTZMER R, SOLOMON J A. Hedgehog pathway inhibition for the treatment of basal cell carcinoma[J]. Target Oncol, 2019, 14(3): 253-267. DOI: 10.1007/s11523-019-00648-2.

(收稿:2025-08-10;修回:2025-10-19)

(编辑 严 涵)